Soils and Foundations 2014;54(4):845–858

HOSTED BY

ELSEVIER

CrossMark

The Japanese Geotechnical Society

Soils and Foundations

www.sciencedirect.com
journal homepage: www.elsevier.com/locate/sandf

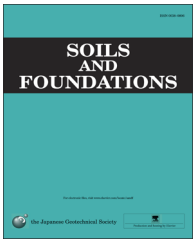

Stress–dilatancy relationships of sand in the simulation of volumetric behavior during cyclic torsional shear loadings

Laddu Indika Nalin De Silva[a,c], Junichi Koseki[b,*], Seto Wahyudi[c], Takeshi Sato[d]

[a]Department of Civil Engineering, University of Moratuwa, Sri Lanka
[b]Institute of Industrial Science, University of Tokyo, Japan
[c]Department of Civil Engineering, University of Tokyo, Japan
[d]Integrated Geotechnology Institute Ltd., Japan

Received 22 December 2011; received in revised form 7 April 2014; accepted 26 April 2014
Available online 31 July 2014

Abstract

In order to describe the volumetric behavior of soil subjected to shearing, a relationship that deals with the ratio of plastic strain increments to stress ratio (i.e. a stress–dilatancy relationship) is required in addition to the stress–shear strain relationship. In view of the above, stress–dilatancy relationships during cyclic torsional shear loadings were experimentally investigated in the current study. Based on the experimental results, a bilinear non-unique stress–dilatancy model was proposed for stress controlled drained cyclic torsional shear loading. The stress–dilatancy relationships during virgin loading and subsequent cyclic loading were modeled separately by considering the effects of stress history (over-consolidation or normal consolidation). Then the volume change of Toyoura sand specimens subjected to cyclic torsional shear loading was simulated by combining the simulation of stress–shear strain relationship with the proposed stress–dilatancy relationships. It was observed from the comparison of the experiment results with the simulation of volumetric strain that, after combining with accurate modeling of stress–shear strain relationship, the proposed stress–dilatancy relationship can reasonably simulate the volumetric behavior of sand subjected to various drained cyclic torsional shear loadings.

Keywords: Stress–dilatancy relationship; Drained cyclic shear; Volumetric behavior of sand; Hollow cylindrical torsional shear test

1. Introduction

When subjected to shearing, sand particles slide over each other and rearrange, causing dilation of the material. Depending on the density and stress history, dilation can be either positive or negative.

Volumetric strain increment during undrained loading is usually assumed to consist of two major components namely, volumetric strain increment due to dilatancy and volumetric strain increment due to consolidation/swelling. In order to propose a model to reasonably predict the cyclic undrained behavior or liquefaction of sand, one essential requirement is to propose a model to reasonably predict the volumetric behavior of sand due to dilatancy.

For the above purpose, a relationship between the ratio of plastic volumetric strain increment to plastic shear strain increment and the stress ratio (i.e. a stress–dilatancy relationship) is required in addition to stress–shear strain relationship

*Corresponding author.
E-mail addresses: nalinds@uom.lk (L.I.N. De Silva), koseki@iis.u-tokyo.ac.jp (J. Koseki), seto-w@iis.u-tokyo.ac.jp (S. Wahyudi), tsato@iis.u-tokyo.ac.jp (T. Sato).
Peer review under responsibility of The Japanese Geotechnical Society.

http://dx.doi.org/10.1016/j.sandf.2014.06.015

Nomenclature

$\tau_{z\theta}$ shear stress
σ_z, σ_r and σ_θ axial, radial and circumferential stresses, respectively
p' mean effective stress during torsional shear loading
p_c' the maximum value of mean effective stress ever applied
$\tau_{z\theta}/p'$ shear stress ratio
$\gamma_{z\theta}^p$ and ε_{vol}^p plastic shear strain and plastic volumetric strain, respectively
$d\gamma_{z\theta}^p$ and $d\varepsilon_{vol}^p$ plastic shear strain increment and plastic volumetric strain increment, respectively
$-d\varepsilon_{vol}^p/d\gamma_{z\theta}^p$ dilatancy ratio
R_k gradient of the empirical stress–dilatancy relationship
R_{max} the maximum value of R_k
C intercept of the empirical stress–dilatancy relationship
C_{min} minimum value of C
D_m plastic shear moduli immediately after reversal of stress/initial plastic shear moduli (i.e. damage parameter)
OC over-consolidation ratio

and thus investigated in the current study. This relationship can be further related to the flow rule for plastic modeling (i.e., the relationship between plastic strain increment ratio and stress ratio: refer Muir Wood, 1990 among others for details), which would be employed for more general purposes.

Various forms of stress–dilatancy relationships have been proposed based on various theoretical bases for different loading conditions such as triaxial and plane strain loading. Among them, the most commonly employed stress–dilatancy relations are originally based on energy principles assuming a purely frictional slipping mechanism.

Rowe (1962, 1969) and Rowe et al. (1964) derived stress–dilatancy relations for triaxial compression, triaxial extension and plane strain conditions by assuming that the granular material can be represented by a regular packing of spheres or cylinders and the ratio of energy increment input to the output to the granular media is a constant (K). Some other widely known stress–dilatancy relationships include the sliding block theory (Tokue, 1978; Moroto, 1987; among others), Roscoe's energy dissipation equation (Roscoe et al.,1963) and Taylor's energy dissipation equation (Taylor, 1948). It should be noted that all the above stated stress–dilatancy relations were originally developed for monotonic loading conditions.

Pradhan et al. (1989) experimentally investigated the stress–dilatancy relations of Toyoura sand subjected to cyclic triaxial and cyclic torsional shear loadings on isotropically consolidated specimens and concluded that a unique stress–dilatancy relationship, which is rather independent of the specimen density, the type of stress path, the stress history, the pressure level or so, was obtained only for dilatancy rates in terms of the ratio of the plastic shear strain increment $d\gamma_{z\theta}^p$ and the plastic volumetric strain increment $d\varepsilon_{vol}^p$ due solely to $d\gamma_{z\theta}^p$. In addition, they have reported that the stress–dilatancy relationships in the beginning of virgin loading in triaxial tests are significantly affected by the over-consolidation history of sand, while the effect of over-consolidation vanishes with subsequent cyclic loading. It was also reported that, as a result of reversal of direction of loading, the rate of dilatancy ($-d\varepsilon_{vol}^p/|d\gamma_{z\theta}^p|$) changes discontinuously. Based on the above experimental investigation, Pradhan and Tatsuoka (1989) modified some available stress–dilatancy relationships based on the sliding block theory, Rowe's theory, Roscoe's energy dissipation theory and Taylor's energy dissipation theory to apply for cyclic triaxial and torsional shear loading conditions. It was concluded that, after the proposed modifications are applied, some of the above theories can well simulate the stress–dilatancy relations under drained cyclic triaxial and torsional loading conditions.

However, it should be noted that, compared to the various theoretical proposals for stress–dilatancy relationships, limited experimental investigations can be found in the literature. This may be partly due to the technical difficulties involved in obtaining reliable and high resolution volume change measurements. Limited experimental investigations include Pradhan and Tatsuoka (1989) who obtained stress–dilatancy relationships of Toyoura sand by employing a high-sensitive electronic balance to measure the volume change of specimens. Shahnazari (2001) also experimentally investigated stress–dilatancy relationships of Toyoura sand under different loading conditions. Balakrishnaiyer (2000) obtained the stress–dilatancy relationship of Chiba gravel subjected to cyclic triaxial loading.

Pradhan and Tatsuoka (1989) reported their experimental data of Toyoura sand in cyclic torsional shear, and showed that two unique empirical relationships of shear stress over mean effective stress ($\tau_{z\theta}/p'$) versus dilatancy ratio ($-d\varepsilon_{vol}^p/d\gamma_{z\theta}^p$) for $d\tau_{z\theta}>0$ and $d\tau_{z\theta}<0$ could be derived. Nishimura (2002) employed the above empirical stress–dilatancy relationships to model the drained and undrained cyclic behavior of sand by assuming a unique linear combination of ($\tau_{z\theta}/p'$) versus ($-d\varepsilon_{vol}^p/d\gamma_{z\theta}^p$). He further showed that the stress–dilatancy relationships during virgin loading and subsequent cyclic loadings are different hence modeled them using different linear equations. In addition, it was observed that the effects of over-consolidation significantly alter the stress–dilatancy relationship during virgin loading. However, limited attempts have been made to address the effects of over-consolidation on stress–dilatancy relationships.

In view of the above background, stress–dilatancy relationships during cyclic torsional shear loadings were experimentally investigated in the current study. In addition, the applicability of empirical stress–dilatancy equation as

Table 1
Test conditions and stress paths.

Test	Dr_{ini} (%)	Stress paths
SAT 30	78.6	1. IC ($\sigma'_z=\sigma'_r=\sigma'_\theta=50\rightarrow100$ kPa) (**$OC=1$**) 2. ITS ($\tau_{z\theta}=0\rightarrow60\rightarrow-60\rightarrow0$ kPa, 9 cycles at $\sigma'_z=\sigma'_r=\sigma'_\theta=100$ kPa) 3. ITS ($\tau_{z\theta}=0\rightarrow80$ kPa: failure at $\sigma'_z=\sigma'_r=\sigma'_\theta=100$ kPa)
SAT 35	79.3	1. IC ($\sigma'_z=\sigma'_r=\sigma'_\theta=50\rightarrow100$ kPa) (**$OC=1$**) 2. ITS ($\tau_{z\theta}=0\rightarrow60\rightarrow-60\rightarrow0$ kPa, 10 cycles at $\sigma'_z=\sigma'_r=\sigma'_\theta=100$ kPa)
SAT 11	77.9	1. IC ($\sigma'_z=\sigma'_r=\sigma'_\theta=50\rightarrow400\rightarrow100$ kPa) (**$OC=4$**) 2. ITS ($\tau_{z\theta}=0\rightarrow60\rightarrow-60\rightarrow0$ kPa, 5 cycles at $\sigma'_z=\sigma'_r=\sigma'_\theta=100$ kPa)
SAT 12	78.5	1. IC ($\sigma'_z=\sigma'_r=\sigma'_\theta=50\rightarrow400\rightarrow100$ kPa) (**$OC=4$**) 2. ITS ($\tau_{z\theta}=0\rightarrow40\rightarrow-40\rightarrow50\rightarrow-50\rightarrow60\rightarrow-60\rightarrow70\rightarrow-70\rightarrow80$ kPa: failure, $\sigma'_z=\sigma'_r=\sigma'_\theta=100$ kPa)
SAT 17	56.8	1. IC ($\sigma'_z=\sigma'_r=\sigma'_\theta=50\rightarrow400\rightarrow100$ kPa, 11 cycles) (**$OC=4$**) 2. ITS ($\tau_{z\theta}=0\rightarrow50\rightarrow-40\rightarrow50\rightarrow-50\rightarrow60\rightarrow-60\rightarrow75$ kPa: failure, $\sigma'_z=\sigma'_r=\sigma'_\theta=100$ kPa)

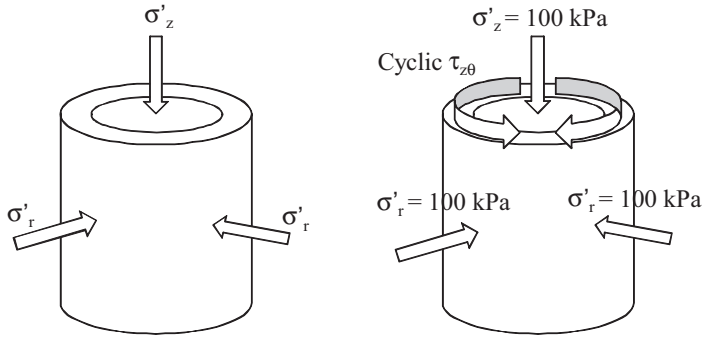

IC loading
(Isotropic Consolidation and swelling, i.e. $\sigma'_z=\sigma'_r=\sigma'_\theta$ with no shear stress)

ITS loading
(Isotropic Torsional Shear loading, i.e. $\sigma'_z=\sigma'_r=\sigma'_\theta=100$ kPa with cyclic shear stress)

Note: inner and outer cell pressure values were kept equal throughout the test. Hence, $\sigma'_r=\sigma'_\theta$

Dr_{ini}: relative density (%), measured at an isotropic stress state of $\sigma'_c=30$ kPa.
Isotropic Consolidation. ITS: Cyclic torsional shear loading.
OC=Over-consolidation ratio.

proposed by Nishimura (2002) and Nishimura and Towhata (2004) was investigated. Finally, the proposed stress–dilatancy relationship was combined with the modeling of stress–shear strain relationship of Toyoura sand to simulate the volumetric strain of sand subjected to different drained cyclic torsional shear loadings, and the simulation results were compared with the corresponding experiment data.

2. Test material, apparatus and procedures

Test material used for the current study is air-dried Toyoura sand, a widely tested uniform sand in Japan with sub-angular particles ($D_{50}=0.162$ mm). Sand from "batch H" that has a specific gravity (G_s) of 2.635, maximum void ratio (e_{max}) of 0.966, minimum void ratio (e_{min}) of 0.600 and coefficient of uniformity (U_c) of 1.46 was used to prepare the specimens.

A high-capacity medium-sized hollow cylinder apparatus at Institute of Industrial Science (IIS), The University of Tokyo, was used for the testing program. A similar apparatus with a large deformation capacity was used by Chiaro et al. (2012, 2013) in their study on the large deformation properties of loose saturated Toyoura sand in undrained cyclic torsional shear. Since externally measured deformations in hollow cylindrical specimens are affected by non-uniform deformations of specimens (Xu et al., 2013 among others), a recently developed local deformation measurement technique was employed in the evaluation of quasi-elastic deformation properties in the current study. Refer De Silva et al. (2005) for the details of the torsional shear apparatus and local deformation measurement system used.

A series of drained cyclic torsional shear loading tests were conducted on saturated Toyoura sand specimens. All the specimens prepared were 20 cm in outer diameter, 12 cm in inner diameter and 30 cm in height. A modified air pluviation technique in which pluviation was done in the radial direction while slowly moving the nozzle of the pluviator in alternate clockwise/anticlockwise directions in the current study to minimize the degree of anisotropy of horizontal bedding plane of hollow cylindrical specimens (refer De Silva et al., 2006 for the details). Specimens were prepared to have a relative density between 56% and 80%, which was measured at a confining pressure of 30 kPa. Due to the relatively large size of specimens,

the double vacuum method (Ampadu and Tatsuoka, 1993) was used to saturate the specimens. This ensured a B value greater than 95% in all the specimens tested.

The specimens were subjected to different isotropic stress histories before being subjected to cyclic torsional shear loadings in order to investigate the effects of over-consolidation on stress–dilatancy relationships. Herein, while referring to Ishihara and Okada (1978), the over-consolidation ratio is defined as p'_c/p', where p'_c is the maximum value of the mean effective stress that had been applied to the specimen, and p' is the value of the mean effective stress under which the torsional shear loading was conducted. Small cyclic loadings in axial and torsional directions were applied at different stress levels for the evaluation of quasi-elastic deformation properties of Toyoura sand. Refer Table 1 for the test conditions, the stress paths employed for the tests presented in this paper and a schematic illustration of the stress application sequences.

2.1. Measurement of volume change of specimens

In order to investigate the stress–dilatancy relationships, accurate measurement of the volume change of the specimens is essential. Therefore, high-sensitive electronic balance (Mettler Toledo™, Model PM 360) with a measuring range of 360 g was employed. Since the weight of the beaker and initial amount of water is about 180 g, the effective measuring capacity of the balance is about 180 g ($\varepsilon_{vol}=3\%$ for the specimen size used). The balance can be tared off within this range and the accuracy for the first 60 g is 0.001 g ($\Delta\varepsilon_{vol}=1.66\times10^{-5}\%$ for the specimen size used) with a linearity of ±0.002 g.

Fig. 1 schematically illustrates the volume change measurement system with the electronic balance. The balance cell with a load cell was removed from the original product and installed inside a special pressure chamber. The transfer cable from the cell was connected to the remaining electronic unit and the unit was connected to a computer via RS 232 connection. The balance was calibrated by means of a 100 g dead weight. The pressure that is applied to the pressure chamber during the experiment was kept constant at 200 kPa (back pressure).

Effects of buoyancy force acting on the submerged part of drainage tube was taken into account by using Eq. (1) as proposed by Pradhan et al. (1986).

$$\Delta vol=\left\{1-(d_s/d_b)^2\right\}\times\Delta F/\gamma_w \quad (1)$$

where, Δvol is the true volume change of the specimen, d_s is the outer diameter of the Nylon tube (3 mm), d_b is the inner diameter of the beaker (72 mm), ΔF is the apparent force change as observed by the balance and γ_w is the unit weight of water.

The evaporation of water from beaker can cause some error in the Δvol measurements in experiments that take a long time. In the present study, it takes about two days to complete a test and it was found that the apparent change of volumetric strain for three days due to evaporation is less than 0.003% for the specimen size used. Therefore, volume change due to evaporation was neglected in the current study. In addition, volume change during shearing was unaffected by the effects of membrane penetration in the present study, since the effect of membrane penetration on volume change measurement remained constant during the drained cyclic torsional shearing that was conducted under a constant value of the effective confining stress.

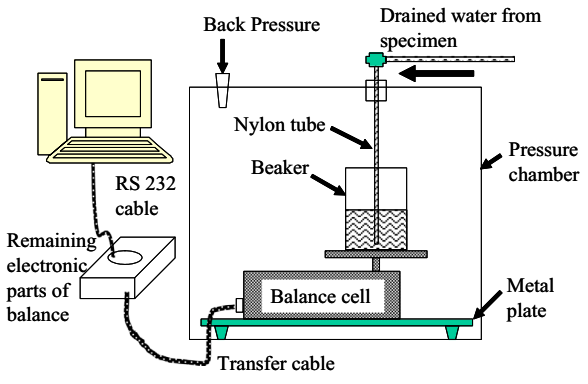

Fig. 1. Volume change measurement system using an electronic balance.

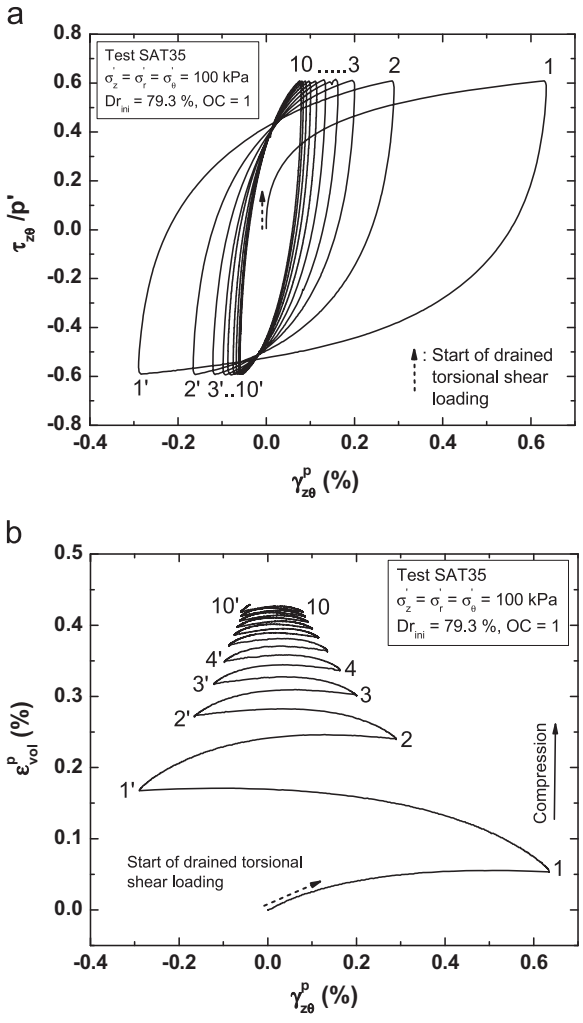

Fig. 2. Results of a normally-consolidated dense specimen with constant stress amplitude; (a) $\tau_{z\theta}/p'$ versus $\gamma^p_{z\theta}$, (b) ε^p_{vol} versus $\gamma^p_{z\theta}$.

3. Volumetric behavior of saturated sand during cyclic torsional shear loading

Normally consolidated and over-consolidated (over-consolidation ratio equal to 4) dense Toyoura sand specimens were subjected to drained cyclic torsional shear loadings in the current study. In addition, over-consolidated loose Toyoura sand specimens were also tested. Fig. 2a shows the typical shear stress over mean effective stress ($\tau_{z\theta}/p'$) versus plastic shear strain ($\gamma^p_{z\theta}$) relationship of a normally-consolidated dense specimen subjected to cyclic torsional shear loadings with constant shear stress amplitude. The plastic volumetric strain (ε^p_{vol}) versus $\gamma^p_{z\theta}$ relationship for the same specimen is shown in Fig. 2b. Plastic strain components were evaluated by deducting the elastic strain components from total strains. The elastic strain components were evaluated by employing the quasi-elastic model (IIS model) proposed by HongNam and Koseki (2008), as summarized briefly in Appendix. The parameters used in the above model for sand specimens tested in the current study are shown in Table 2. It can be seen from Fig. 2b that the specimen shows contractive behavior at the start of loading and becomes dilative after some stress level. When the loading direction was reversed, the specimen suddenly shows contractive behavior. In addition, the accumulated value of ε^p_{vol} and the amplitude of $\gamma^p_{z\theta}$ decreases with subsequent cyclic loadings with constant stress amplitude.

$\tau_{z\theta}/p'$ versus $\gamma^p_{z\theta}$ and ε^p_{vol} versus $\gamma^p_{z\theta}$ relationships for a over-consolidated dense specimen subjected to similar cyclic torsional shear loading as above are shown in Fig. 3a and b, respectively. Initially, the specimen does not show any significant ε^p_{vol} due possibly to the effect of over-consolidation as shown in Fig. 3b. When the shear stress level of the specimen exceeds some value, the specimen tends to show dilative behavior. During subsequent cyclic loadings, the accumulated value of ε^p_{vol} and the amplitude of $\gamma^p_{z\theta}$ decreases as well.

In order to investigate the effect of over-consolidation on the cyclic stress–dilatancy relationship before the volumetric response of the material changes from contractive behavior to dilative behavior (also known as phase transformation stress state (Ishihara et al., 1975)) of dense sand, one test was conducted by applying cyclic torsional shear loadings with increasing stress amplitude, starting initially within the phase transformation stress states in positive and negative shear stress directions (approximately, $|\tau_{z\theta}/p'| \le 0.5$). $\tau_{z\theta}$ versus $\gamma^p_{z\theta}$ and ε^p_{vol} versus $\gamma^p_{z\theta}$ relationships for the above specimen are shown in Fig. 4a and b, respectively. An enlarged portion of the first two cycles of ε^p_{vol} versus $\gamma^p_{z\theta}$ relationship is shown in Fig. 4c. It can be observed that the volume change during the first cycle was less than 0.01%.

$\tau_{z\theta}$ versus $\gamma^p_{z\theta}$ relationship and ε^p_{vol} versus $\gamma^p_{z\theta}$ relationship for an over-consolidated loose specimen subjected to increasing stress amplitude cyclic loading are shown in Fig. 5a and b, respectively. An enlarged portion of the first cycle of ε^p_{vol}versus

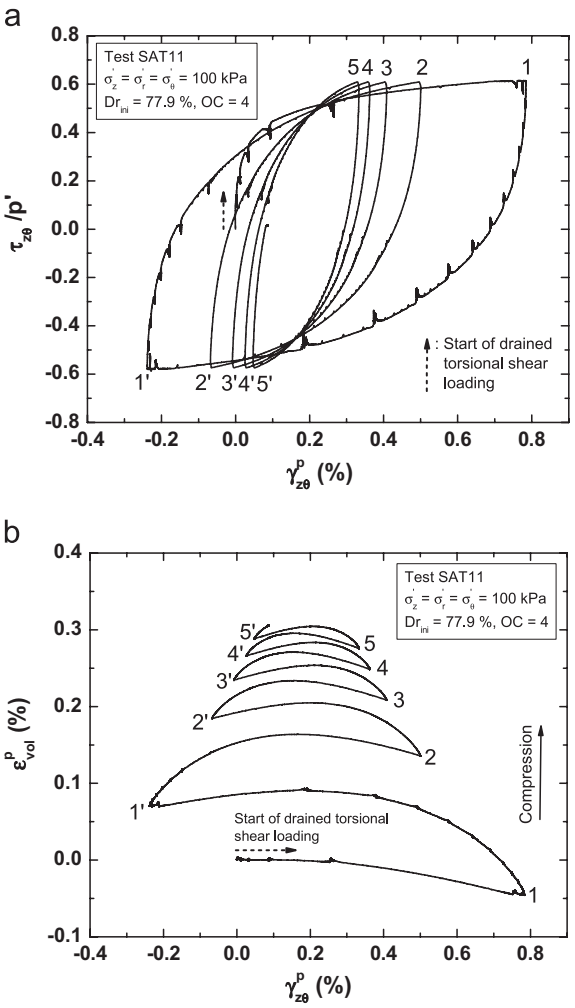

Fig. 3. Results of a over-consolidated dense specimen with constant stress amplitude; (a) $\tau_{z\theta}/p'$ versus $\gamma^p_{z\theta}$, (b) ε^p_{vol} versus $\gamma^p_{z\theta}$.

Table 2
Model parameters.

Test	*Quasi-elastic model parameters*[b]	*Drag parameters*[a]	*Hardening parameter*[a], S_{ult}	*Damage parameter*[a], D_{ult}
SAT 30 SAT 35 SAT 11 SAT 12	E_{zo}=215 MPa, σ'_o=100 kPa, $\nu_{z\theta o}$=0.18, m=0.520, n=0.508, k=0.3, C_E=C_G=0.0, a=0.7	D_1=0.15 D_2=12	1.15	0.2
SAT 17	E_{zo}=190 MPa, σ'_o=100 kPa, $\nu_{z\theta o}$=0.18, m=0.520, n=0.508, k=0.3, C_E=C_G=0.0, a=0.7	D_1=0.01 D_2=3.13		

[a]Drag, hardening and damage parameters are same as those employed in simulating stress–shear strain relationship during drained cyclic torsional shear loading in De Silva and Koseki (2012).

[b]Refer to HongNam and Koseki (2005) for the definition of each parameter.

$\gamma^p_{z\theta}$ relationship are shown in Fig. 5c. The quasi-elastic model parameters used in evaluating the plastic strain components are shown in Table 2. It can be observed that, unlike the volumetric behavior of over-consolidated dense specimens as shown in Figs. 3b and 4b, the over-consolidated loose specimen shows contractive behavior, except in the region immediately after starting the loading.

In all the tests, the volumetric behavior immediately after stress reversal was contractive (Figs. 2b, 3b, 4b and 5b).

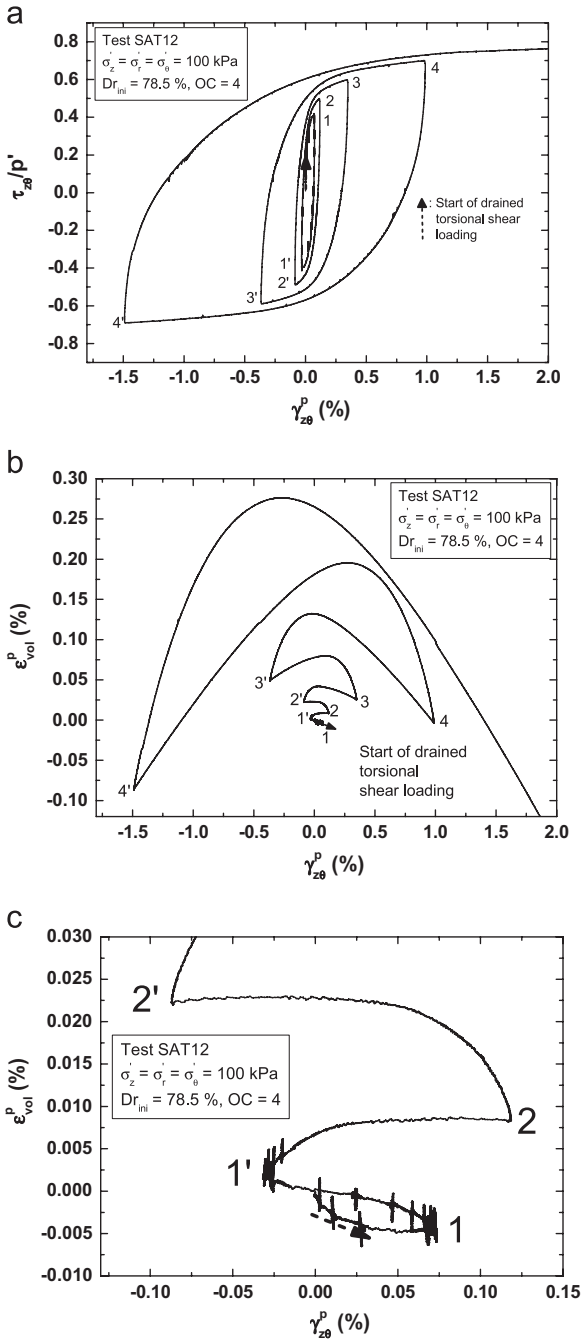

Fig. 4. Results of a over-consolidated dense specimen with increasing stress amplitude; (a) $\tau_{z\theta}/p'$ versus $\gamma^p_{z\theta}$, (b) ε^p_{vol} versus $\gamma^p_{z\theta}$, (c) enlarged portion during start of loading of (b).

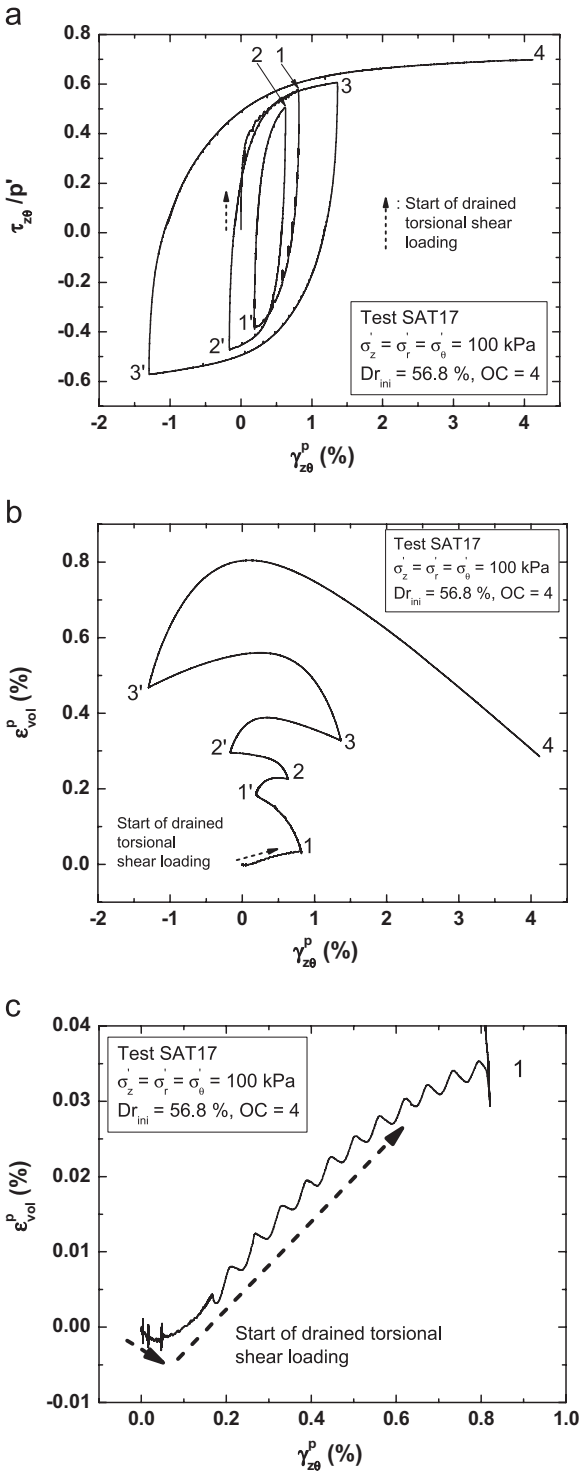

Fig. 5. Results of a over-consolidated loose specimen with increasing stress amplitude; (a) $\tau_{z\theta}/p'$ versus $\gamma^p_{z\theta}$, (b) ε^p_{vol} versus $\gamma^p_{z\theta}$, (c) enlargement of (b).

4. Stress–dilatancy relationships of sand during isotropic torsional shear

Among the many proposals available for stress–dilatancy relationships under various loading conditions, the current study intends to investigate the applicability of stress–dilatancy relationship in terms of shear stress ratio ($\tau_{z\theta}/p'$) versus

dilatancy ratio ($-d\varepsilon^p_{vol}/d\gamma^p_{z\theta}$) for drained cyclic torsional shear loading of sand.

Fig. 6a shows $\tau_{z\theta}/p'$ versus $-d\varepsilon^p_{vol}/d\gamma^p_{z\theta}$ relationship of a normally-consolidated dense specimen subjected to constant amplitude drained torsional shear loading. As has been reported by Nishimura (2002), it can be clearly confirmed in the present study that the stress–dilatancy relationship during virgin loading is different from that of subsequent cyclic loadings. In addition, the above relationship seems to shift slightly to the origin with the progress of cyclic loading as well (note the cyclic numbers shown in Fig. 6a).

Stress–dilatancy relationship for an over-consolidated dense specimen subjected to constant stress amplitude cyclic torsional shear loading is shown in Fig. 6b. It can be seen that the effects of over-consolidation significantly affect the stress–dilatancy relationship during virgin loading and its effects vanish after the stress ratio exceeds the phase transformation stress state (i.e. the stress state at which the volumetric behavior changes from contractive to dilative) as observed by Pradhan and Tatsuoka (1989). In addition, the stress dilatancy relationship shifts slightly to the origin with the subsequent cycles as indicated by cyclic numbers in Fig. 6b.

Stress–dilatancy relationship of the over-consolidated dense specimen, which was subjected to several torsional shear cycles within the phase transformation stress state is shown in Fig. 6c. It is evident in Fig. 6c that, compared to Fig. 6b, not only the virgin loading, but also the subsequent cyclic loadings which were applied within the phase transformation stress state were significantly affected by the effects of over-consolidation. However, the effects of over-consolidation on stress–dilatancy relationship vanish soon after the stress ratio exceeds the phase transformation stress state.

Finally, the stress–dilatancy relationship of an over-consolidated loose sand specimen subjected to increasing stress amplitude cyclic torsional shear loading is shown in Fig. 6d. It can be observed that that the results are similar to those of the over-consolidated dense sand specimen as shown in Fig. 6b. It should be noted that, in all the tests, large absolute values of dilatancy ratios were observed immediately after reversal of stress in both loading and unloading directions.

Based on the above experimental data, the applicability of three different stress–dilatancy models in simulating the volumetric behavior of sand during drained cyclic torsional shear loading was investigated in the current study. These models may be in principle applied for more general stress conditions, including the triaxial one, while no verification could be made due to lack of relevant experimental data. Thus, the applicability of the proposed model is limited at present to the torsional shear loading condition as investigated in the current study.

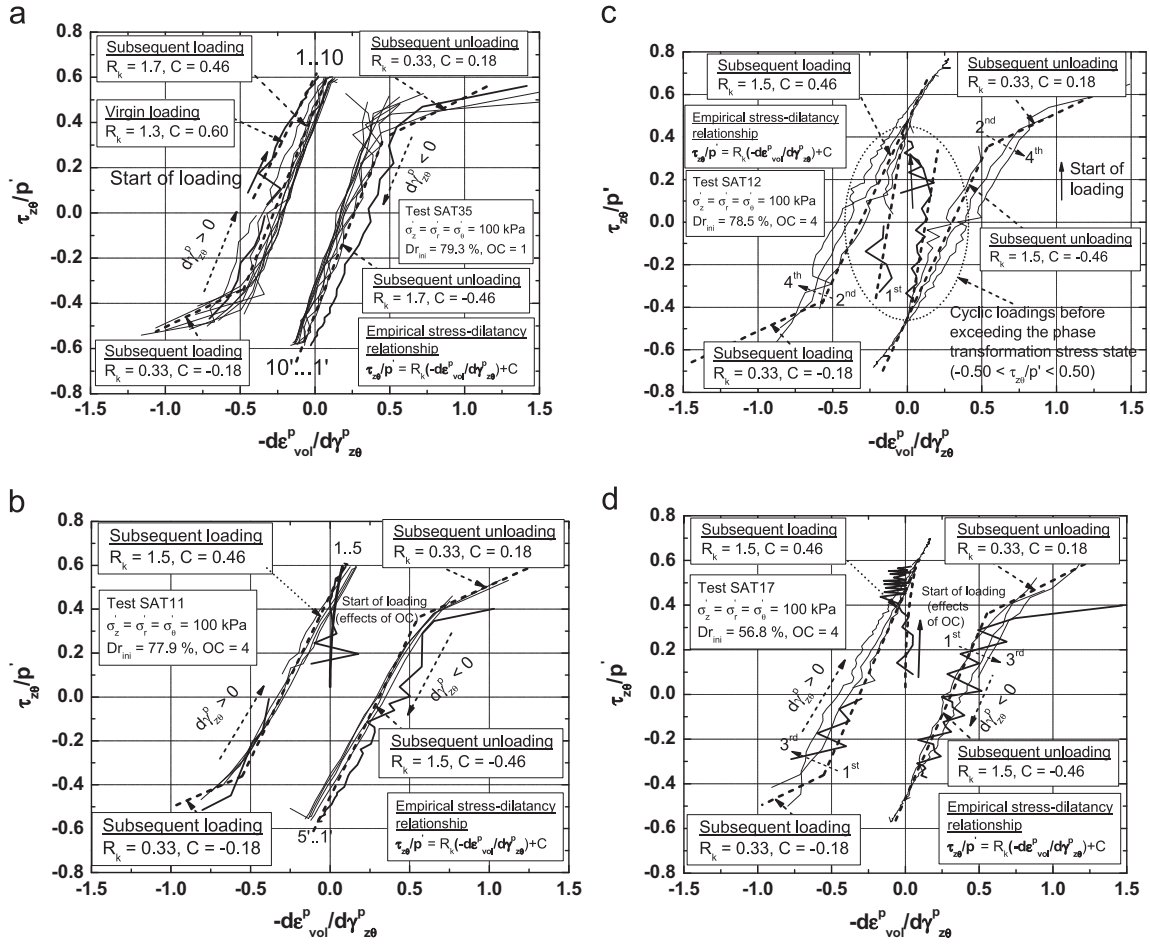

Fig. 6. Stress–dilatancy relationships; (a) normally-consolidated dense specimen, (b) over-consolidated dense specimen, (c) over-consolidated dense specimen with several cycles with increasing stress amplitude, (d) over-consolidated loose specimen.

4.1. Linear stress–dilatancy model

Nishimura (2002) proposed an empirical linear modeling of $\tau_{z\theta}/p'$ versus $-d\varepsilon^p_{vol}/d\gamma^p_{z\theta}$ relationship as shown in Eq. (2). He further showed that the stress–dilatancy relationships during virgin loading and subsequent cyclic loadings are different hence modeled them using different linear equations.

$$\tau_{z\theta}/p' = R_k(-(d\varepsilon^p_{vol}/d\gamma^p_{z\theta})) \pm C \text{ with positive and negative signs of } C \text{ for } d\gamma^p_{z\theta} > 0 \text{ and } d\gamma^p_{z\theta} < 0, \text{ respectively} \quad (2)$$

In the present study, $R_k = 1.5$ and 1.7 were found to be appropriate based on the experimental results as shown in Fig. 6a through d to represent the average stress–dilatancy relationship of subsequent cyclic loadings of over-consolidated and normally-consolidated specimens, respectively. C is the $\tau_{z\theta}/p'$ value at zero dilatancy (i.e., the value of shear stress ratio at phase transformation), which was found to be within 0.4 and 0.5. Therefore, an average value for $C = 0.46$, which is similar to the value employed by Nishimura (2002), was employed in the current study. The R_k and C values for the stress–dilatancy relationship during normally consolidated virgin loading are taken as 1.3 and 0.6, respectively. The stress–dilatancy relationship during virgin loading of an over-consolidated specimen will be discussed later.

4.2. Bi-linear stress–dilatancy model

As discussed before, significantly larger absolute values of dilatancy ratios could be observed immediately after the reversal of loading direction as shown in Fig. 6a through d. This may have been caused by damage to soil particle structure or stress-induced anisotropy by the preceding loading history. Thorough investigation on the above would be necessary to explain or estimate further detailed physical mechanisms at the background of such peculiar response.

Similar response was observed and reported by Pradhan et al. (1989) (one may refer to Figs. 11 and 13 of their paper, for example). However, the number of data plots was too limited to reveal general trend of behavior, which is possibly affected by different resolutions and time intervals of data sampling between their study and the present study.

In order to take such a response into account, the stress–dilatancy relationship immediately after the reversal of loading direction was approximated by another average linear combination of $\tau_{z\theta}/p'$ versus $-d\varepsilon^p_{vol}/d\gamma^p_{z\theta}$ as given in Eq. (2) by employing $R_k = 0.33$ and $C = -0.18$.

In addition, it is assumed that the stress–dilatancy relationship would follow the above linear relationship immediately after the stress reversal until it intersects with and follows the linear relationship discussed in the previous section. The combination of two linear equations will be repeated for subsequent cyclic loadings. The proposed bi-linear stress–dilatancy model is illustrated for each experimental data (refer to the dashed lines) as shown in Fig. 6a through b.

The stress–dilatancy relationship for virgin loading for normally consolidated sand is modeled by the linear relationship as described before.

4.3. Modified bi-linear stress–dilatancy model

In order to obtain a more realistic simulation of ε^p_{vol}, the variations in the stress–dilatancy relationship as can be observed in Fig. 6a through d, where C and R_k values slightly vary with cyclic loading need to be taken into account. Note that the C values during constant stress amplitude cyclic torsional loading can become smaller than 0.46 with subsequent cyclic loadings, as seen in Fig. 6a and b, possibly due to the effects of stiffening (subsequent decrease in accumulated plastic strain during the previous reloading/re-unloading branch, as shown in Figs. 2a and 3a).

Furthermore, it is evident from the experimental results as seen in Fig. 6c and d that C value may even become larger than 0.46, possibly due to the damage caused by large amplitude cyclic torsional loading depending on the accumulated plastic strain during the previous reloading/re-unloading branch.

Similarly, the R_k value can also vary. However, it is reasonable to assume that the values of C and R_k cannot vary indefinitely since there is an upper limit for the damage to the soil structure due to the formation of the shear band at large strain levels. Limited experimental evidence also suggests that the values of C and R_k vary between a certain range, as seen in Fig. 6a through d.

Considering the above factors, the bilinear stress–dilatancy model as proposed before was further modified, as shown in Eq. (3), to take into account the slight variations of R_k and C by introducing a damage factor D_m formulated as shown in Eq. (4). The experimental evidence shown in Fig. 7 suggests that the damage factor D_m can be expressed as a function of accumulated plastic shear strain between current and the previous turning points during cyclic loadings. In the proposed Eq. (3), R_k is replaced by $R_{max} \times D_m$ to account for the slight variation in R_k value and C is replaced by C_{min}/D_m to account for the slight variation in C. R_{max} is taken as the maximum possible value for R_k and C_{min} is taken as the minimum possible value for C. Note that D_m is as same as the damage factor as proposed by De Silva and Koseki (2012), which takes into account the damage to the plastic shear moduli during drained large cyclic torsional shear loadings (refer Fig. 7). The proposed stress–dilatancy relationship is expressed in Eq. (3).

$$\frac{\tau_{z\theta}}{p'} = (R_{max} \times D_m) \times \left(-\frac{d\varepsilon^p_{vol}}{d\gamma^p_{z\theta}}\right) \pm \frac{C_{min}}{D_m} \quad (3)$$

$$D_m = \frac{(1+e^{-0.8})(1-D_{ult})}{1+e^{\left\{\left(\left|\Delta\gamma^p_{z\theta}\right|_p\right)-0.8\right\}}} + D_{ult} \quad (4)$$

where R_{max} is the maximum value of R_k in Eq. (2) ($R_{max} = 1.5$ and 1.7 was selected based on the experimental evidence for

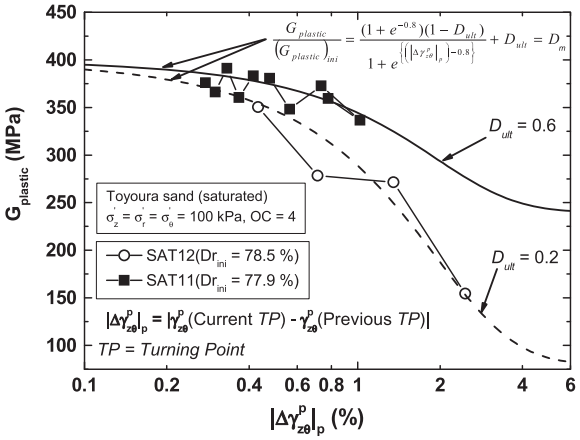

Fig. 7. Damage to plastic shear moduli at large stress levels and proposed empirical equation to estimate the damage factor, D_m.

over-consolidated and normally consolidated specimens, respectively).

C_{min} is the minimum value of C after application of large number of constant stress amplitude cyclic loadings (C_{min}= 0.36 was used for both over-consolidated and normally consolidated specimens).

D_m is the plastic shear modulus in the beginning of each reload and re-unload that was normalized with the initial plastic shear modulus (refer Fig. 7). D_m is equal to unity at the beginning of initial loading with $|\Delta\gamma^p_{z\theta}|_p=0$; otherwise D_m is reduced to a positive value smaller than unity; thus, this parameter is herein called the "damage factor" for short.

D_{ult} is the minimum value of D_m, which corresponds to the minimum value of normalized plastic shear modulus (refer Fig. 7 for the details).

$|\Delta\gamma^p_{z\theta}|_p$ is the total plastic strain in percent induced between the current and previous turning points.

e=2.718 (the base of natural logarithms).

Note that, since the values of $R_{max}\times D_m$ and C_{min}/D_m cannot be varied indefinitely, as discussed above, the variation in the above values has been restricted to a certain range as governed by the following boundary conditions, by referring to the experimental data of the current study, the results of Nishimura (2002) and the results of Pradhan and Tatsuoka (1989) (it should be noted that the above researchers did not consider the slight variations of R_k and C in their studies and employed a kind of average values for R_k and C).

$R_{max}\times D_m$ should be greater than 1.0 (when $R_{max}\times D_m$ became less than 1.00, $R_{max}\times D_m$=1.00 was used).

C_{min}/D_m should be less than 0.50 (when C_{min}/D_m became greater than 0.50, C_{min}/D_m=0.50 was used).

Therefore, the $R_{max}\times D_m$ value in Eq. (3) varies between 1.5 and 1.7–1.0 and the C_{min}/D_m value varies between 0.36 and 0.50 depending on the accumulated plastic strain between the current and previous turning points (i.e. damage parameter, D_m).

Note that Nishimura (2002) employed an average R_k value of 1.15 and C value of 0.46 in their study. Since clear experimental evidence is available to support the value of the damage factor D_m as shown in Fig. 7, the values for R_{max} and C_{min} were selected in the current study by considering the possible range of variations of R_k and C as observed in the experimental data of the current study and Nishimura (2002) and the results of Pradhan and Tatsuoka (1989).

Note that the above modifications were applied only to the portion of the bilinear stress–dilatancy relationship, which shows a steeper response before the reversal of loading direction. Since effects of cyclic loading history on the stress–dilatancy relationship immediately after the reversal of the loading direction is rather insignificant, the stress–dilatancy relationships immediately after the stress-reversal, shown in Fig. 6a through d, was not modified (i.e. R_k=0.33 and C=−0.18).

4.4. Effects of over-consolidation in stress–dilatancy relationship

As discussed before, the effects of over-consolidation significantly alter the stress–dilatancy relationship during virgin loading and its effects vanish after some stress state. Oka et al. (1999) proposed the following stress–dilatancy equation to consider the effects of over-consolidation. The same equation was employed in the current study, which is given as follows:

$$\left(-\frac{d\varepsilon^p_{vol}}{d\gamma^p_{z\theta}}\right) = D_k\left(\frac{\frac{\tau_{z\theta}}{p'} - \left(\frac{\tau_{z\theta}}{p'}/\ln(OC)\right)}{R_k}\right) \quad (5)$$

where

$$D_k = \left[\frac{\tau_{z\theta}}{p'}/(C\times\ln(OC))\right]^{1.5}$$

where OC is the over-consolidation ratio. The values of R_k=1.3 and C=0.6, which are same as those used in the stress–dilatancy relationship during virgin loading of a normally consolidated specimen are used in the above equation. Since the effects of over-consolidation on stress–dilatancy relationship vanish once the shear stress ratio exceeds a certain value, it is assumed that the stress–dilatancy relationship during virgin loading of over-consolidated specimens follows Eq. (5) until it meets Eq. (2) with R_k=1.3 and C=0.6 (refer Fig. 8 for an illustration) and then follow the respective stress–dilatancy model (either linear, bi-linear or modified bi-linear) as discussed in previous sections.

Some typical curves proposed by Eq. (5) for different constant OC values are shown in Fig. 8. According to Eq. (5), if OC=2.718, there would be no volume change ($-d\varepsilon^p_{vol}/d\gamma^p_{z\theta}$ =0) of the specimen until the stress state exceeds the phase transformation stress state of a normally consolidated specimen (refer Fig. 8). If $OC<2.718$, the volumetric behavior of the specimen during virgin loading is always contractive according to Eq. (5). On the other hand, if $OC>2.718$, the volumetric behavior of the specimen during virgin loading is always dilative. This seems to be consistent with the observed behavior of the over-consolidated dense specimens (OC=4, Dr_{ini}=80%) tested in the current study as shown in Figs. 3b and 4b. As shown in Fig. 6b and c, the stress–dilatancy relationship during virgin loading reasonably follows Eq. (5) with OC=4.

In contrast to the above, over-consolidated loose specimen tested under the same over-consolidation ratio as above shows

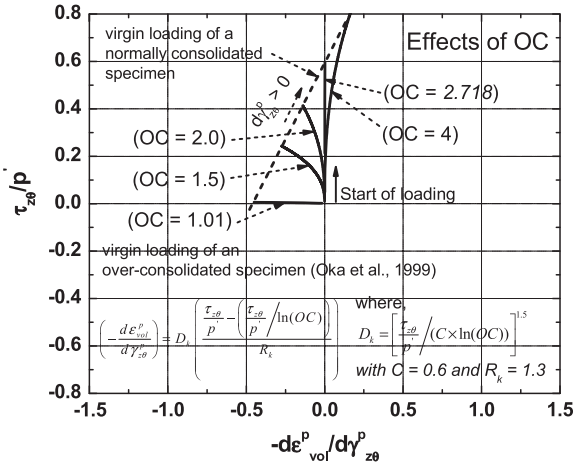

Fig. 8. Stress–dilatancy relationship during virgin loading of an over-consolidated specimen (Oka et al., 1999).

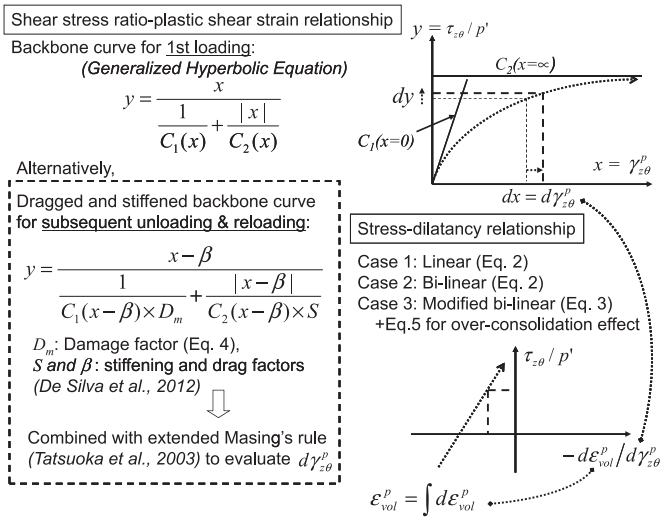

Fig. 9. A schematic illustration of the simulation of ε^p_{vol}.

contractive behavior during virgin loading, as shown in Fig. 5b. It can be seen in Fig. 6d that the curve proposed by Eq. (5) with $OC=4$ does not follow the experimental results during virgin loading of loose over-consolidated specimen tested in the current study. Therefore, Eq. (5) may need further modification for use with over-consolidated loose specimens.

The above observations suggest that the volumetric behavior of sand due to shearing is not only affected by over-consolidation ratio but also its density. Therefore, using only a constant value for OC during shearing may not be appropriate. While noting such limitations, as described above, Eq. (5) is employed in the subsequent simulation of volumetric behavior.

5. Simulation of volumetric behavior of sand during drained cyclic torsional shear loadings

$\tau_{z\theta}/p'$ Versus $\gamma^p_{z\theta}$ relationship (hence $d\gamma^p_{z\theta}$) can be obtained by following the modeling proposed by De Silva and Koseki (2012). Then $d\gamma^p_{z\theta}$ is substituted into the stress–dilatancy relationships, as discussed in the preceding sections, to evaluate $d\varepsilon^p_{vol}$. Hence, as schematically shown in Fig. 9, ε^p_{vol} can be evaluated by numerical integration and the $\tau_{z\theta}/p'$ versus ε^p_{vol} relationship can be evaluated.

It is suggested in De Silva and Koseki (2012) that a better simulation of the $\tau_{z\theta}/p'$ versus $\gamma^p_{z\theta}$ relationship can be obtained after introducing the stiffening behavior of sand during cyclic loading and damage to plastic shear modulus at large stress levels into extended Masing's rules as proposed by Tatsuoka et al. (2003). In view of the above, as summarized briefly in Fig. 9, the same simulation procedure was employed in the current study to evaluate $d\gamma^p_{z\theta}$. A simulation of volumetric strain was carried out by substituting $d\gamma^p_{z\theta}$ into the three empirical stress–dilatancy relationships as discussed in the preceding section. A comparison of experimental results with its simulation is presented for three cases. In Case 1, simulation was carried out by employing the linear stress–dilatancy model as proposed by Nishimura (2002). The bilinear stress–dilatancy model was employed in Case 2. Finally, the simulation was carried out by employing the modified bilinear stress–dilatancy model as shown in Case 3.

Comparison of $\tau_{z\theta}/p'$ versus ε^p_{vol} relationship of a normally consolidated specimen subjected to constant stress amplitude cyclic loading with its simulation is shown in Fig. 10a through d. Experimental evidence shows a reduction in the accumulation of ε^p_{vol} with the subsequent cyclic loading as shown in Fig. 10a. In addition, significant volume change is accumulated during the first cycle as well. This observation is not well simulated in Case 1 and Case 2 simulations, as shown in Fig. 10b and c. However, the simulation significantly improved in Case 3 after considering the change in stress–dilatancy relationship as observed during constant stress amplitude cyclic loading. As shown in Fig. 10d, both significant volume change during the first cycle and reduction in the accumulation of ε^p_{vol} with the subsequent cyclic loading could be reasonably simulated.

A similar comparison for a typical over-consolidated specimen subjected to constant stress amplitude cyclic loading is made in Fig. 11a through c. It can be seen that the simulation improves after introducing the modified bilinear stress–dilatancy model as shown in Fig. 11c, where relatively large accumulation of ε^p_{vol} up to the second cyclic loading could be reasonably simulated. It should also be noted that, by considering the effect of over-consolidation by employing Eq. (5), slightly dilative behavior as observed during the first quarter cycle (i.e., during virgin loading) could be reasonably simulated as well.

Fig. 12a through d shows a comparison of the $\tau_{z\theta}/p'$ versus ε^p_{vol} relationship with its simulation for an over-consolidated specimen subjected to increasing stress amplitude cyclic loadings. The sudden increase in volume change observed soon after the stress reversal at large stress levels is reasonably simulated in Fig. 12d after employing the modified bilinear stress–dilatancy relationship. However, it should be noted that there is no significant difference between Case 1 and Case 2 simulations for all the tests discussed so far in the current study. This may be due to the fact that the simulation of plastic shear strain increment ($d\gamma^p_{z\theta}$) soon after the reversal of loading direction is very small; hence, the $d\varepsilon^p_{vol}$ values evaluated by applying linear or bilinear stress–dilatancy relationships make no significant difference in volumetric strain evaluations.

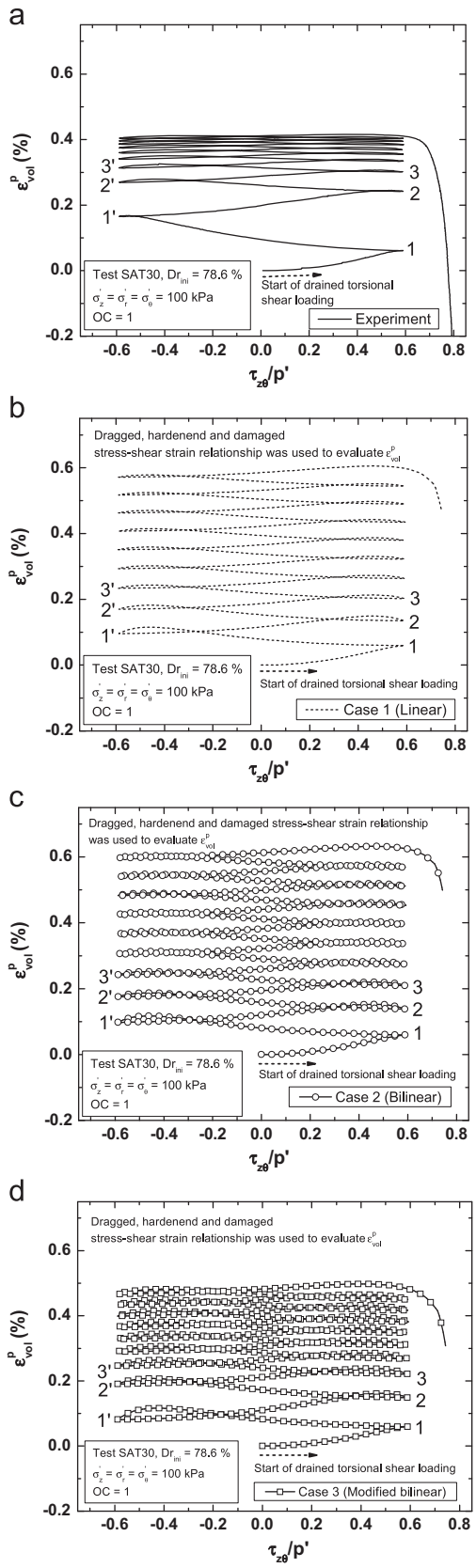

Fig. 10. Volumetric strain of a normally-consolidated dense specimen subjected to constant stress–amplitude cyclic loading; (a) experimental results, (b) simulation using linear stress–dilatancy model, (c) simulation using bi-linear stress–dilatancy model, (d) simulation using modified bi-linear stress–dilatancy model.

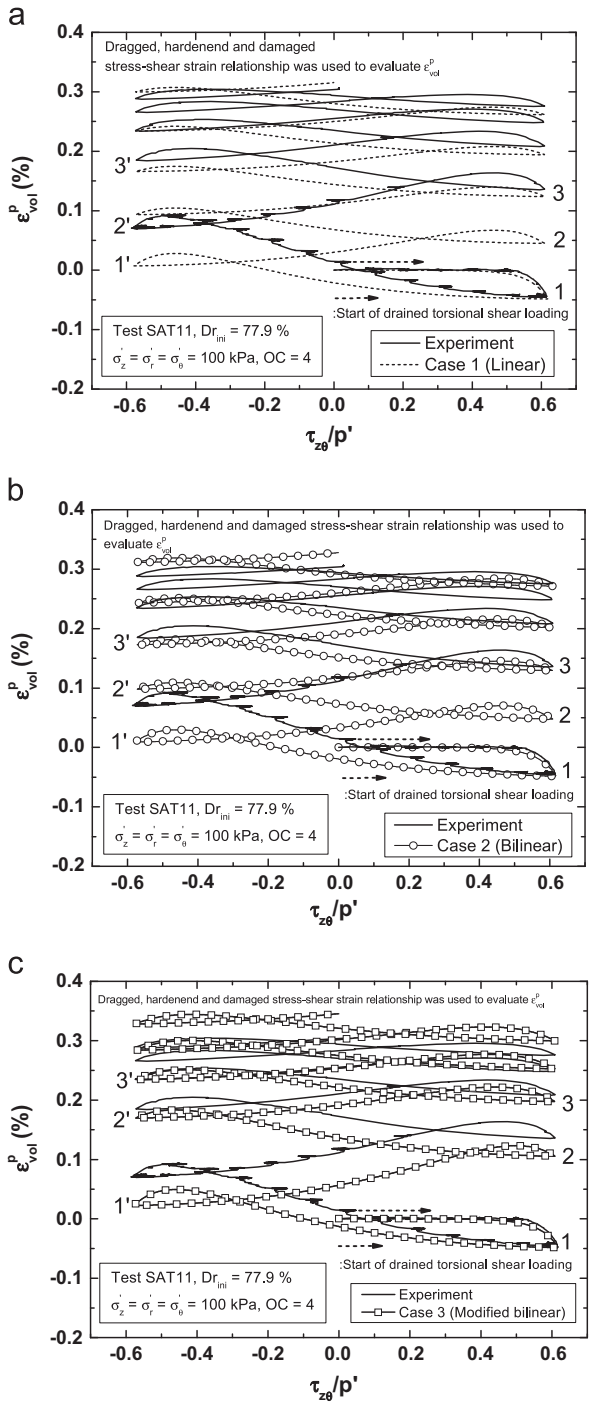

Fig. 11. Comparison of volumetric strain of a over-consolidated dense specimen subjected to constant stress–amplitude cyclic loading with its simulation using; (a) linear stress–dilatancy model, (b) bi-linear stress–dilatancy model, (c) modified bi-linear stress–dilatancy model.

A comparison of the $\tau_{z\theta}/p'$ versus ε^p_{vol} relationship with its simulation for a loose over-consolidated specimen is shown in Fig. 13a through d. First, the simulation of volumetric strain during virgin loading was done by using Eq. (4) with $OC=4$. The simulation during subsequent cyclic loadings was done by applying linear unique stress–dilatancy model. It can be seen that, as discussed before, the simulation during virgin loading shows dilative behavior while the experimental results show

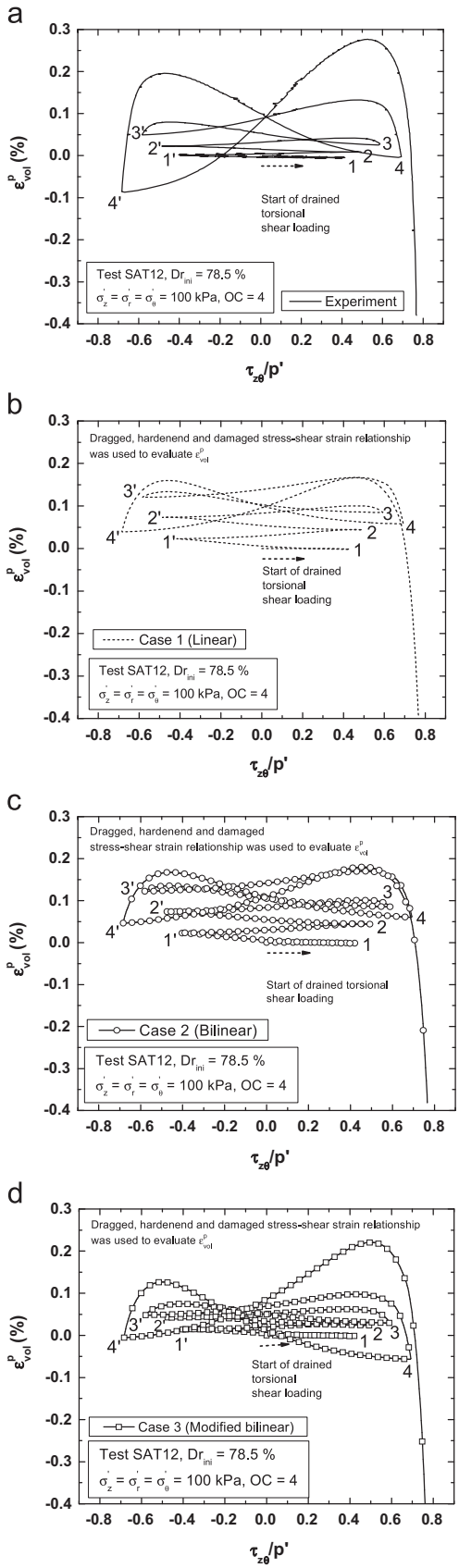

Fig. 12. Volumetric strain of a over-consolidated dense specimen subjected to varying amplitude cyclic loading; (a) experimental results, (b) simulation using linear stress–dilatancy model, (c) simulation using bi-linear stress–dilatancy model, (d) simulation using modified bi-linear stress–dilatancy model.

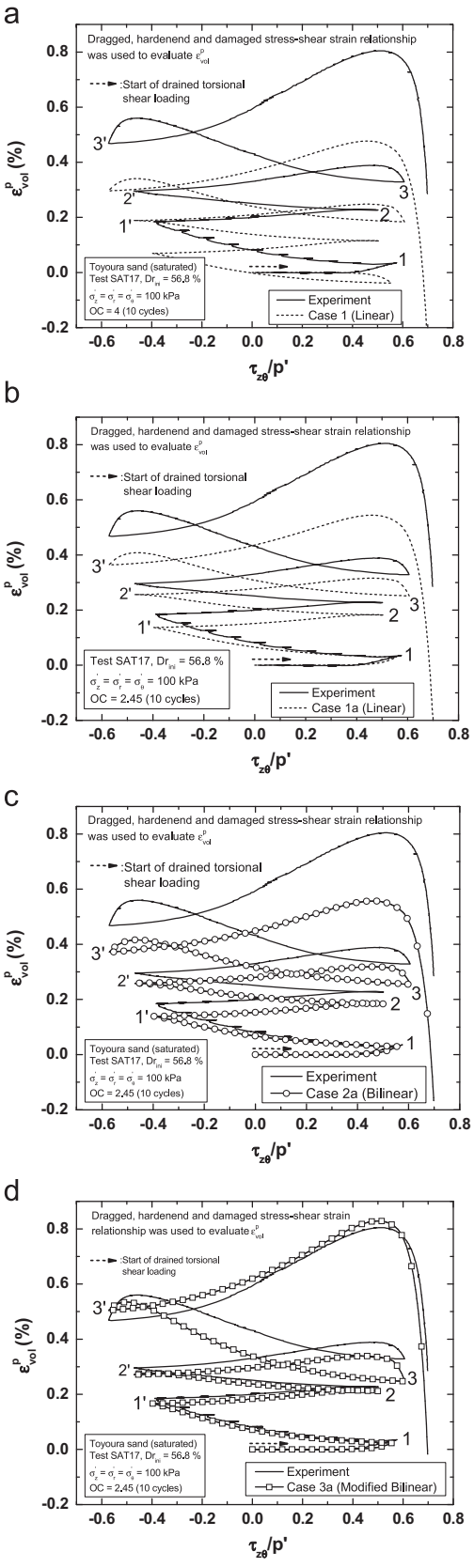

Fig. 13. Comparison of volumetric strain of a over-consolidated loose specimen subjected to varying amplitude cyclic loading with its simulation using; (a) linear stress–dilatancy model (with $OC=4$), (b) linear stress–dilatancy model (with $OC=2.45$), (c) bi-linear stress–dilatancy model (with $OC=2.45$), (d) modified bi-linear stress–dilatancy model (with $OC=2.45$).

contractive behavior. Therefore, in order to obtain a better simulation, an average constant OC value of 2.45, which is less than 2.718 was used in the current study. It can be seen in Fig. 13b that the simulation of volumetric strain during virgin loading is significantly improved as a result of the above modification and agrees well with the experimental results. However, the simulation of volumetric strain by using linear or bilinear stress–dilatancy models during subsequent cyclic loading does not reasonably fit with the experimental results as shown in Fig. 13b and c. The simulation is significantly improved after the modified bilinear stress–dilatancy relationship is introduced into the simulation of volumetric strain during subsequent cyclic loadings as shown in Fig. 13d.

6. Conclusions

Based on the experiment results and simulation of volumetric behavior of sand during cyclic torsional shear loading, the following conclusions can be drawn from the current study.

1) As has been reported in past relevant study, the stress–dilatancy relationship during virgin loading and subsequent cyclic loadings were confirmed to differ from each other. In addition, the effects of over-consolidation significantly alter the stress–dilatancy relationship during virgin loading and its effects vanish after the shear stress ratio exceeds some value. Therefore, the stress–dilatancy relationship during virgin loading was modeled separately by considering the effects of stress history.
2) The empirical linear stress–dilatancy relationship as employed by Nishimura (2002) was further modified based on the experimental evidence into a bilinear stress–dilatancy relationship to represent the stress–dilatancy relationship immediately after stress reversal. In addition, in order to consider the observed changes in the stress–dilatancy relationship during subsequent cyclic loadings, a modified bi-linear stress–dilatancy model was proposed for cyclic torsional shear loading in the current study.
3) No significant difference was observed in the simulation of plastic volumetric strain ε^p_{vol} for linear and bi-linear stress–dilatancy relationships. However, the simulation of ε^p_{vol} was significantly improved and in reasonable agreement with experimental results when the modified bi-linear stress–dilatancy relationship was employed in the simulation of ε^p_{vol}.
4) In the simulation, effect of over-consolidation on the stress–dilatancy relationship during virgin loading was considered by adopting the equation proposed by Oka et al. (1999). A reasonable simulation could be made on the volumetric behavior of dense sand, while some modification was required in simulating the volumetric behavior of loose sand.

Acknowledgments

Our special appreciation goes to Dr. T. Honda, Takenaka Research & Development Institute, Japan, for developing the user friendly Windows™ based control program for the medium-sized hollow cylindrical apparatus used for laboratory testing in the current study. In addition, the authors sincerely acknowledge the Ministry of Education, Culture, Sports, Science and Technology, Japan (Grant no. 21360221) for providing the financial assistance for the current research.

Appendix

During torsional shear loading applied in the present study, axial, radial and circumferential stresses ($\sigma'_z, \sigma'_r, \sigma'_\theta$) were kept constant and only $\tau_{z\theta}$ was applied. Therefore, $\gamma^e_{z\theta}$ could be evaluated by employing the following equation. Its applicability on Toyoura sand has been verified for stress states with a shear stress ratio $\tau_{z\theta}/p'$ in the range of -0.6 and $+0.6$ under both loading and unloading conditions (HongNam and Koseki, 2005), which generally cover the stress states employed in the present study. A similar type of modeling has been adopted by many other researchers as summarized for example by Mitchell and Soga (2005).

$$d\gamma^e_{z\theta} = \frac{1}{G_{z\theta}} d\tau_{z\theta} \tag{A1}$$

$$G_{z\theta} = \frac{f(e)}{f(e_o)} \frac{G_{z\theta o}}{\sigma'^n_o} (\sigma'_z \sigma'_\theta)^{n/2} (1 - C_G k_n^2) \tag{A2}$$

where

$f(e)$ is the void ratio function ($f(e)=(2.17-e)^2/(1+e)$) (Hardin and Richart, 1963); $G_{z\theta o}$ is the initial shear modulus at the initial isotropic stress of σ'_o, which was evaluated from the initial Young's modulus (E_{zo}) in the present study; n is the stress state dependency parameter for shear modulus; σ'_z and σ'_θ are axial and circumferential stresses; C_G is a damage parameter for shear modulus; and k_n is defined as follows (Yu and Richart, 1984):

$$k_n = (\sigma'_1/\sigma'_3 - 1)/[(\sigma'_1/\sigma'_3)_{max} - 1] \tag{A3}$$

where

$(\sigma'_1/\sigma'_3)_{max}$ denotes the principal stress ratio at failure, i.e. peak principal stress ratio.

The elastic shear strain $\gamma^e_{z\theta}$ can be evaluated by the numerical integration of Eq. (A1). Then the plastic shear strain $\gamma^p_{z\theta}$ could be evaluated by subtracting the elastic shear strain from the total shear strain $\gamma_{z\theta}$.

References

Ampadu, S.K., Tatsuoka, F., 1993. Effects of setting of setting method on the behavior of clays in triaxial compression from saturation to undrained shear. Soils Found. 33 (2), 14–34.

Balakrishnaiyer, K., 2000. Modeling of Deformation Characteristics of Gravel Subjected to Large Cyclic Loading (Ph.D. thesis). Dept. of Civil Engineering, The University of Tokyo, Japan.

Chiaro, G., Koseki, J., Sato, T., 2012. Effects of initial static shear on liquefaction and large deformation properties of loose saturated Toyoura sand in undrained cyclic torsional shear tests. Soils Found. 52 (3), 498–510.

Chiaro, G., Kiyota, T., Koseki, J., 2013. Strain localization characteristics of loose saturated Toyoura sand in undrained cyclic torsional shear tests with initial static shear. Soils Found. 53 (1), 23–34.

De Silva, L.I.N., Koseki, J., Sato, T., Wang, L., 2005. High capacity hollow cylinder apparatus with local strain measurements. In: Proceedings of the

Second Japan–U.S. Workshop on Testing, Modeling and Simulation, Geotechnical Special Publication, ASCE, vol. 156, pp. 16–28.

De Silva, L.I.N., Koseki, J., Sato, T., 2006. Effects of different pluviation techniques on deformation property of hollow cylinder sand specimens. In: Proceedings of International Symposium on Geomechanics and Geotechnics of Particulate Media, Ube, Yamaguchi, Japan, pp. 29–33.

De Silva, L.I.N., Koseki, J., 2012. Modeling of sand behavior in drained cyclic shear. In: Miura, S. (Ed.), Advances in Transportation Geotechnics II. CRC Press, Netherlands, pp. 686–691.

Hardin, B.O., Richart Jr., F.E., 1963. Elastic wave velocities in granular soils. J. Soil Mech. Found. Div. ASCE, 89; 33–65.

HongNam, N., Koseki, J., 2005. Quasi-elastic deformation properties of Toyoura sand in cyclic triaxial and torsional loadings. Soils Found. 45 (5), 19–38.

HongNam, N., Koseki, J., 2008. Deformation characteristics of dry Toyoura sand in large cyclic torsional loading and their modeling. In: Burns, Mayne, Santamarina (Eds.), Proceedings of the Fourth International Symposium on Deformation Characteristics of Geomaterials, vol. 2. IS Atlanta, USA, pp. 801–807.

Ishihara, K., Tatsuoka, F., Yasuda, S., 1975. Undrained deformation and liquefaction of sand under cyclic stresses. Soils Found. 15 (1), 29–44.

Ishihara, K., Okada, S., 1978. Yielding of overconsolidated sand and liquefaction model under cyclic stresses. Soils Found. 18 (1), 57–72.

Mitchell, J.K., Soga, K., 2005. Fundamentals of Soil Behavior, 3rd edition John Wiley & Sons, USA (p. 450).

Moroto, N., 1987. On deformation of granular material in simple shear. Soils Found. 27 (1), 77–85.

Muir Wood, D., 1990. Soil Behavior and Critical State Soil Mechanics. Cambridge University Press, UK, USA (p. 227).

Nishimura, S., 2002. Development of Three Dimensional Stress–Strain Model of Sand Undergoing Cyclic Undrained Loading and Stress-axes Rotation (M. Eng thesis). Dept. of Civil Engineering, The University of Tokyo, Japan.

Nishimura, S., Towhata, I., 2004. A three-dimensional stress–strain model of sand undergoing cyclic rotation of principal stress axes. Soils Found. 44 (2), 103–116.

Oka, F., Yashima, A., Tateishi, Y., Taguchi, Y., Yamashita, S., 1999. A cyclic elasto-plastic constitutive model for sand considering a plastic-strain dependence of the shear modulus. Geotechnique 49 (5), 661–680.

Pradhan, T.B.S., Tatsuoka, F., Molenkamp, F., 1986. Accuracy of automated volume change measurement by means of a differential pressure transducer. Soils Found. 26 (4), 150–158.

Pradhan, T.B.S., Tatsuoka, F., 1989. On stress–dilatancy equations of sand subjected to cyclic loading. Soils Found. 29 (1), 65–81.

Pradhan, T.B.S., Tatsuoka, F., Sato, Y., 1989. Experimental stress–dilatancy relations of sand subjected to cyclic loading. Soils Found. 29 (1), 45–64.

Roscoe, K.H., Schofield, A.N., Thurairajah, A., 1963. Yielding of clays in states wetter than critical. Geotechnique 13 (3), 211–240.

Rowe, P.W., 1962. The stress–dilatancy relation for static equilibrium of an assembly of particles in contact. Proc. R. Soc. Lond. Ser. A 269, 500–527.

Rowe, P.W., Barden, L., Lee, I.K., 1964. Energy components during the triaxial tests and direct shear tests. Geotechnique 14 (3), 247–261.

Rowe, P.W., 1969. The relation between the shear strength of sands in triaxial compression, plane strain and direct shear. Geotechnique 19 (1), 75–86.

Shahnazari, H., 2001. Experimental Investigation on Volume Change and Shear Deformation Characteristics of Sand Undergoing Cyclic Loading (Ph.D. thesis). Department of civil engineering, The University of Tokyo, Japan.

Tatsuoka, F., Masuda, T., Siddiquee, M.S.A., Koseki, J., 2003. Modeling the stress–strain relations of sand in cyclic plane strain loading. J. Geotech. Geoenviron. Eng., 129. ASCE450–467.

Taylor, D.W., 1948. Fundamentals of Soil Mechanics. John Wiley, New York.

Tokue, T., 1978. A consideration about Rowe's minimum energy ratio principal and a new concept of shear mechanism. Soils Found. 18 (1), 1–10.

Xu, B., Nakai, K., Noda, T., Takaine, T., 2013. A three-dimensional soil–water coupled FE analysis of hollow cylinder test concerning non-uniform deformation. Soils Found. 53 (6), 923–936.

Yu, P., Richart Jr., F.E., 1984. Stress ratio effects on shear modulus of dry sands. J. Geotech. Eng. ASCE 110 (3), 331–345.